Thread as a Versatile Material for Low-Cost Microfluidic Diagnostics

Xu Li, Junfei Tian, and Wei Shen*

Australian Pulp and Paper Institute, Department of Chemical Engineering, Monash University, Clayton Campus, VIC 3800 Australia

ABSTRACT This paper describes a new and simple concept for fabricating low-cost, low-volume, easy-to-use microfluidic devices using threads. A thread can transport liquid via capillary wicking without the need of a barrier; as it is stainable, it is also a desirable material for displaying colorimetric results. When used in sewing, threads have 3D passageways in sewed materials. The wicking property and flexibility of thread make it particularly suitable to fabricate 3D microfluidic devices. Threads can also be used with other materials (e.g., paper) to make microfluidic devices for rapid qualitative or semiquantitative analysis. These thread-based and thread-paper-based devices have potential applications in human health diagnostics, environmental monitoring, and food safety analysis, and are particularly appropriate for the developing world or remote areas, because of their relatively low fabrication costs.

KEYWORDS: thread • paper • diagnostics • 3D microfluidics • low-cost sensors.

New concepts and applications of low-cost, portable, and field-based diagnostic technologies have become an area attracting a lot of research interest (1). The potential of these technologies in providing affordable healthcare and environmental monitoring to remote and developing regions strongly drives the continuous developments of these technologies. The recent rise of paper-based microfluidic devices (2−5) once again shows the attraction of low-cost and field-based technologies.

Cotton thread as an ancient material in civilization is also an attractive material for the fabrication of low-cost and low-volume microfluidic diagnostic devices for healthcare and environmental assays. This is because that the gaps between fibers provide capillary channels for liquids to wick along the thread. Thread has been used for sensor fabrication, but only for purposes other than building microfluidic sensors. The idea of using electronic threads for human health monitoring has been reported in many studies (6−9). The electronic threads are usually metal-based threads (7) or threads made by carbon nanotubes coated with polyelectrolytes (8, 9). To the best of our knowledge, there has been no work reported using cotton or other multifilament threads for fabricating simple and low-cost microfluidic analytical devices.

In this study, cotton thread is used to fabricate microfluidic devices with 3D structures by sewing it onto other materials (e.g., polymer film). In this way, we show the possibility to fabricate high density thread microfluidic channels to enable the transportation of several liquids through the structure without mixing. Threads with different wettability can also be used to manipulate liquid wicking and mixing. These capabilities further enable us to fabricate 3D thread-based microfluidic devices which encompass complicated microfluidic channels compared to lateral flow systems (5). The fabrication of thread-based microfluidic devices is simple and relatively low-cost, because it requires only sewing needles or household sewing machines, which are commonly used and affordable, even in some of the under-developed regions. Liquids can penetrate from thread into other hydrophilic porous materials; therefore, thread can be used with other materials (e.g., paper) to form microfluidic devices with enhanced sample delivering efficiency. In this work, thread-based and thread-paper-based microfluidic sensors are fabricated with the incorporated colorimetric indicators for two important biomarkers for several human medical conditions, nitrite ion (NO_2^-) and uric acid (UA) (10−12). The potential of using thread and thread-paper microfluidic sensors to provide low-cost, low-volume, semiquantitative, and multispecies analysis is shown through the detection and measurement of these species. Our results demonstrate that thread is a suitable material for fabricating microfluidic diagnostic devices for monitoring human health, environment and food safety; especially for the population in less-industrialized areas or remote regions (13, 14).

Experimental Section. Cotton thread was kindly provided by the School of Fashion and Textiles, RMIT University, Melbourne, Australia. The average diameter of the thread was measured using a microscope (Olympus, BX-60) that was interfaced to a PC to allow object size measurement. The cotton thread was found to have an average thickness of 244 ± 41 μm. Natural cotton thread is not wettable by aqueous liquids; this is because natural cotton fibers have wax on their surface and in the fiber wall. Therefore, natural cotton thread needs to be dewaxed or surface treated to allow the wicking of aqueous liquids (15). In this study, to obtain hydrophilic cotton thread, we used a vacuum plasma reactor (K1050X plasma asher (Quorum

* Corresponding author. Tel: +61 3 99053447. Fax: +61 3 99053413. E-mail: wei.shen@eng.monash.edu.au.
Received for review September 11, 2009 and accepted November 27, 2009

DOI: 10.1021/am9006148

Table 1. Surface Atomic Concentration of C and O of Untreated and Treated Threads

sample	filter paper (cellulose)	thread (untreated)	thread (plasma treated)	binding energy (eV)	assignment
C (1 + 2)	0.215	0.784	0.562	285.0, 285.5	C−C, C−H
C (3)	0.605	0.163	0.261	286.8	C−O
C (4)	0.180	0.032	0.107	288.3	O−C−O, C═O
C (5)		0.021	0.069	289.2	O−C═O
O	0.596	0.139	0.574	533.2	

Emitech, UK)) to treat cotton thread for 1 min at an intensity of 50 W. The vacuum level for the treatment was 6×10^{-1} mbar.

The treated and untreated thread samples were analyzed using XPS to show the effect of the plasma treatment on their surface chemistry and wettability differences. XPS analysis was conducted using an AXIS HSI spectrometer (Kratos) with monochromatized Al Kα radiation. The photoelectron emission angle was 90° with respect to the sample surface. This corresponds to a maximum sampling depth of ca. 10 nm. Thread samples were wound around a sample holder to form a closely packed mesh providing the necessary area for the X-ray beam, which was about 2 mm in diameter. Table 1 lists the changes in surface atomic concentration of C and O before and after plasma treatment. Filter paper was used as the control for cellulose. The presence of C (1 + 2) on filter paper surface was most likely due to surface contamination during the production and packaging processes. Plasma treatment may have two effects on the thread surface modification: First, the surface was substantially oxidized; this is indicated by the increase in surface concentration of C species with binding energies of 288.3 and 289.2 eV, which correspond to the generation of surface O−C−O, C═O and O−C═O groups. Second, the increase in surface concentration of C−O (286.8 eV) may mean that the plasma treatment also partially removed wax and exposed the underlying cellulose. These combined changes significantly increased the surface oxygen concentration (Table 1) and therefore increased surface polarity. The increased water wettability after plasma treatment is consistent with the surface chemistry changes revealed by XPS. After treatment, water can readily wet and wick along the cotton thread.

To characterize the hydrophobic and hydrophilic contrast between threads, we prepared a series of water−isopropyl alcohol (IPA) (HPLC grade, EMD Chemicals Inc.) solutions with different IPA mass percentages (14, 16, 18, 20, 22, and 24%) as a means to measure the onset of wicking of water−IPA solutions in untreated cotton thread. Because the surface tension values of the water−IPA system are known (16), it can be used as a convenient measure to characterize the wicking property of the thread. Aspler et al. (17) and Nisbet et al. (18) have shown that the polar liquid wicking in a porous material occurs when the surface tension of the liquid is lowered to a critical value. The wicking onset, in the porous material, can be identified by testing the wicking speed of a series of liquids with different surface tension values. Although high surface tension liquids do not wick (zero speed) in the material, liquids that have a certain surface tension value start to wick in the material at an observable speed. Aspler et al. (17) referred this surface tension value as the critical wicking surface tension. Liquids that have a surface tension lower than this value can all wick in the material. This method was used to identify the liquid wicking onset of untreated cotton thread.

Millipore-purified water was used to prepare all aqueous samples required for testing the performance of threads. The ink solutions (cyan, magenta, blank and yellow) used in the liquid wicking experiments were prepared by diluting commercial Canon ink jet inks (CLI Y-M-C-BK, PGBK (http://www.canon.com.au/)) with water. The red ink solution was prepared by mixing magenta and yellow ink solutions. The green ink solution was a mixture of cyan and yellow ink solutions. The density values of the ink solutions were measured using a Mettler Toledo Densito 30Px (Switzerland). The surface tension of the ink solutions were measured by the capillary rise method (19) using a cathetometer. Glass capillary tubes were first washed with laboratory detergent (RBS 35 detergent, Chemical Products, Belgium), followed by rinsing with ample amounts of water. The capillary tubes were dried under ambient temperature, followed by 60 °C oven drying. Finally, the tubes were plasma treated to ensure complete wetting. The tube diameter was determined by measuring the capillary raise of n-hexadecane (Aldrich, >99%) of known surface tension.

The stock solution of NO_2^- (10.0 mmol/L) was prepared by dissolving 69.0 mg of sodium nitrite (≥99%, Sigma-Aldrich) in 100 mL water. This stock solution was then diluted with water to get serially diluted NO_2^- standard solutions with concentrations of 1000, 500, 250, 125, and 0 μmol/L. The indicator solution for NO_2^- contained 50 mmol/L sulfanilamide (≥99%, Sigma-Aldrich), 330 mmol/L citric acid (≥99.5%, Sigma-Aldrich), and 10 mmol/L N-(1-naphthyl) ethylenediamine (≥98%, Sigma-Aldrich) (10).

The UA stock solution (10.0 mmol/L) was prepared by dissolving 168.1 mg of uric acid (≥99%, Sigma-Aldrich) in 100 mL o NaOH solution (0.2 mol/L). The UA sample solution (1000 μmol/L) was prepared by further diluting the stock solution with NaOH solution. The indicator solution for UA consisted of a 1:1 ratio mixture of solution A (2.56% (w/v) 2,2′-biquinoline-4,4′-dicarboxylic acid disodium salt hydrate, ≥98%, Sigma-Aldrich) and solution B (20 mmol/L sodium citrate and 0.08% (w/v) copper(II) sulfate, ≥99%, Sigma-Aldrich) (10).

Results and Discussion. Gaps between fibers of cotton threads provide capillary channels for liquids to wick along threads without the need of an external pump. Panels A and B in Figure 1 show two examples of using plasma-treated hydrophilic threads to form 3D structures. In Figure

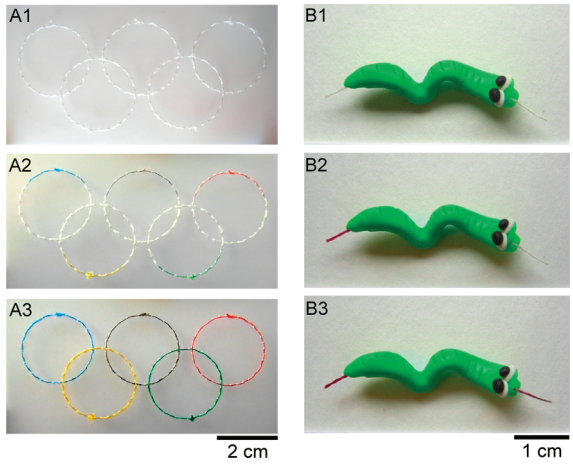

FIGURE 1. (A) Three-dimensional microfluidic pattern fabricated by sewing threads onto a translucent polymer film. (A1) Pattern sewed using hydrophilic cotton threads; (A2) introduction of liquids on threads; (A3) liquids wick throughout the thread pattern. Their stitches cross one another from above and below the polymer film and therefore do not mix. (B) Three-dimensional microfluidic channel of thread imbedded in plasticine. (B1) Imbedded hydrophilic cotton thread in plasticine; (B2) introduction of a liquid on the thread from one end; (B3) liquid wicks along the thread through plasticine.

1A, a 3D microfluidic pattern was fabricated by sewing threads through a polymer film. A translucent polymer film was chosen to visually demonstrate the liquid wicking passageways. In this pattern, the stitches of the threads pass one another from above and below the polymer film, and therefore, do not have contact. Ink solutions of different colors wick along the threads and cross one another without mixing. Thus, threads allow complex continuous 3D microfluidic channels to be built without the need of patterned barriers to define the liquid wicking passageways. High-density thread circuitries can be built in a relatively small space that is suitable for miniaturization. Fabrication of such 3D microfluidic structures with threads requires only some basic tools such as a sewing needle or a household sewing machine, and is therefore less reliant on sophisticated equipment required for patterned paper devices. Figure 1B shows ink solution transport through a cotton thread embedded in plasticine. The ink solution can wick through tortuous passageways, even if the solid material enclosing the thread is not wettable by the wicking liquid. Therefore, when thread is used to provide the capillary driving force for liquid transport, the wetting property of the support material will no longer be a design restriction.

Thread has other interesting properties that can be used to control liquid wicking along it. First, liquid wicking along a thread is controlled by the liquid wettability of thread. The hydrophilic–hydrophobic contrast of the treated and untreated thread provides a convenient option to manipulate liquid transport. The wicking onset characterization using the water-IPA solution series showed that solutions of less than 20% IPA (w/w) form bead on the surface of untreated thread and do not wick along the thread. The surface tension value of this solution is 31.2 mN/m at 20 °C (16). IPA solutions of higher concentrations than 20% can wick along the untreated thread. Therefore, aqueous solutions with a surface

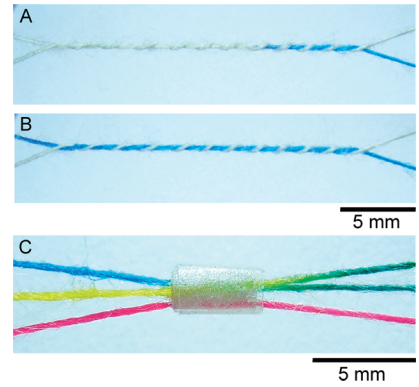

FIGURE 2. (A, B) Twisted pair of an untreated and a plasma-treated cotton thread. When the liquid is introduced onto the treated and hydrophilic thread, the liquid wicks only along the hydrophilic thread. (C) Sample mixing zone demonstrating the manipulation of liquid wicking along threads. The top and the middle threads that transport cyan and yellow liquids are twisted and sleeved inside a heat shrink tube; the bottom thread that transports magenta liquid is not twisted with the other two threads and passes through the mixing zone from outside of the heat shrink tube.

tension higher than 31.2 mN/m can wick only along the treated thread, but not along untreated thread.

The sensitivity of liquid wicking to the surface condition of a thread can be used as a convenient option for designing a thread network to facilitate and control liquid transport. Panels A and B in Figure 2 show a twisted pair of cotton threads, one untreated and the other plasma-treated. The cyan ink solution was introduced onto the treated hydrophilic thread and wicked only along this thread. The surface tension values of all the diluted ink solutions were higher than the critical wicking surface tension of the untreated thread (e.g., the cyan ink solution (10%, v/v) was 37.4 mN/m at 20 °C with the density of 1.022 g/mL). Therefore, the ink solutions can only wick along the treated thread, but not along the untreated thread. Second, liquid wicking can be relayed from a hydrophilic thread to another hydrophilic thread or a hydrophilic porous material. This property of thread makes it possible to use thread with other porous materials to form more sophisticated microfluidic systems. If two hydrophilic threads are twisted together, and a different liquid solution is introduced to each of the thread, the two solutions will mix when the two threads meet. Figure 2C demonstrates a simple mixing zone in a thread device. Three threads pass through a liquid mixing zone, restrained by a tube of sticky tape. The top and the middle threads that transport cyan and yellow ink solutions are twisted and sleeved inside a heat shrink tube; the bottom thread that transports magenta ink solution is not twisted with the other two threads and passes through the mixing zone from outside of the heat shrink tube. The magenta ink solution therefore does not mix with other solutions. The ability to manipulate liquid transport and mixing offers the possibility of using threads to fabricate more sophisticated microfluidic patterns.

Liquids wicking on two twisted hydrophilic threads can mix surprisingly well (Figure 2C). This phenomenon may be related to the good alignment of closely packed long fibres in a thread in a helical arrangement. The fiber gaps, there-

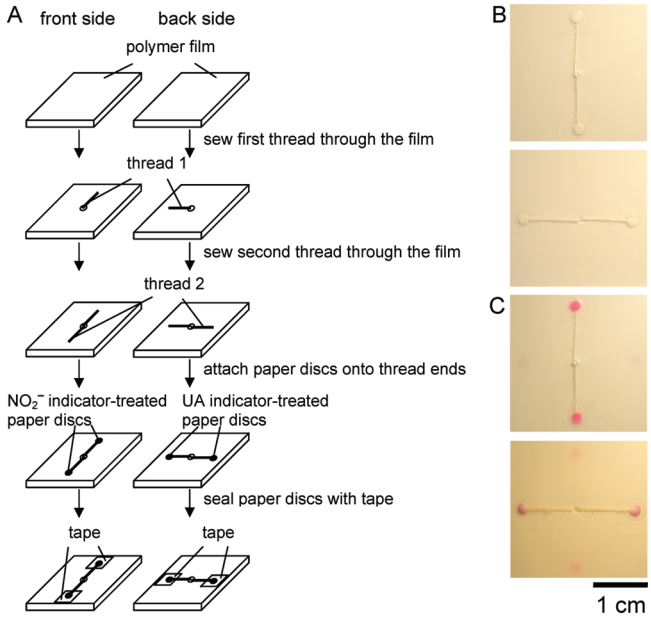

FIGURE 3. Demonstration of a 3D thread-paper microfluidic sensor. (A) Fabrication of the sensor. (B) Front side and back side of the sensor. (C) Different color development on the front side (pink) and back side (purple) of the sensor when multianalyte test solution (500 μM NO_2^-, 500 μM UA) was introduced from the central hole of the sensor onto the two threads and penetrated into paper discs (detection zones).

fore, also have good alignment in the thread. When two threads are twisted together for a number of turns, fiber gaps in one thread are in contact with all fiber gaps of the other thread, and these contacts form new gaps for the liquid to wick. We think the full contact of all fiber gaps between the two twisted threads is responsible for the good liquid mixing result.

Combining the thread properties shown in Figures 1 and 2, multianalyte and 3D microfluidic devices can be easily designed. The combination of thread and filter paper provides a proof-of-concept design for 3D microfluidic devices (Figure 3). Circular paper discs (Ø = 2 mm) were produced from Whatman No.4 filter paper using a disk punching device (Facit 4070, Sweden) to make thread-paper sensors. Paper discs were immersed either in the NO_2^- or the UA indicator solution respectively to full saturation and were then dried in an oven at 60 °C for ~ 5 min. Two hydrophilic cotton threads (~2 cm) were sewed through an opaque polymer film (2.5 cm × 2.5 cm), with half the length left on the front side and the other half on the back side of film. The ends of the two threads on the front side were made to contact the two paper discs treated with NO_2^- indicator solution; the other ends of the two threads on the back side were made to contact the paper discs treated with UA indicator solution. Single-sided sticky tape was used to fix the paper discs and threads onto the film (panels A and B in Figure 3). A test solution containing 500 μmol/L NO_2^- and 500 μmol/L UA was prepared by mixing equal volumes of 1000 μmol/L NO_2^- and 1000 μmol/L UA solutions. A 3 μL test solution was introduced onto the threads from the central film hole with a micro pipet (eppendorf research 1.0−10 μL); the test solution rapidly wicked along the threads and reached paper discs. Paper discs treated with NO_2^- indicator on the front side of the film rapidly developed a pink color, confirming the detection of NO_2^-, whereas paper discs treated with UA indicator on the back side of the film developed a purple color, confirming the detection of UA (Figure 3C). The fabrication process of this kind of thread-paper 3D microfluidic devices is simpler than that reported for 3D microfluidic devices fabricated by stacking layers of paper and tape (20).

Thread can be used by itself for semiquantitative colorimetric assay. Cotton thread is white which provides a desirable reference background for colorimetric detections. An aqueous liquid (0.1 μL) wicks for a length of ~6 mm on a plasma-treated household sewing cotton thread which is about the length of two stitches. A thread-based microfluidic device can be made by simply sewing thread onto a support material such as polymer film. For creating NO_2^- calibration curve with thread-based devices, hydrophilic thread was immersed in the NO_2^- indicator solution and was then dried in an oven at 60 °C for ~ 5 min. Five short threads cut from the indicator-treated thread were sewed onto an opaque polymer sheet with one stitch (~3 mm) exposing at the top side of the sheet as the detection zone. Five serially diluted NO_2^- standard solution samples (0.1 μL, 1000, 500, 250, 125, and 0 μmol/L) were deposited onto the five sewed threads separately with a micro pipet (eppendorf research 0.1−2.5 μL). Colorimetric change on each stitch can be clearly seen. The extra amount of solution continues to wick along the thread to the other side of the polymer film and cannot be seen. The color development can be recorded by a digital camera for visual appraisal. Figure 4A shows a photo of three repeated measurements of the same serially diluted NO_2^- solution samples. The results of the colorimetric assays can also be recorded for data analysis with a desktop scanner (Epson Perfection 2450 PHOTO) using the color photo setting and 4800 dpi resolution. It is noted that for the image scanning, the orientation of the stitches should be positioned parallel to the scanning direction of the light bar in the scanner to avoid the shadowing effect caused by the protruding stitches on the polymer film surface. The recorded color image data can then be imported into Adobe Photoshop and converted into grayscale mode. A fixed area is applied to all detection zones. The mean grayscale intensities can be quantified using the histogram function of Adobe Photoshop. The ultimate mean intensity value of each detection zone can be obtained by subtracting the measured average detection zone intensity from the mean intensity of the 0 μmol/L NO_2^- solution; the average intensity data can then be transferred to Microsoft Excel to obtain calibration curve data (Figure 4B). In this work, six independent measurements were taken using six thread-based devices made from the same indicator-treated thread. Data points are the average values ± s.d. (n = 6). Thread, therefore, offers a new design concept for low-cost and low-volume healthcare and diagnostic sensors. The low material cost of such sensors will make them very useful in the developing and remote regions where well-equipped medical services are lacking.

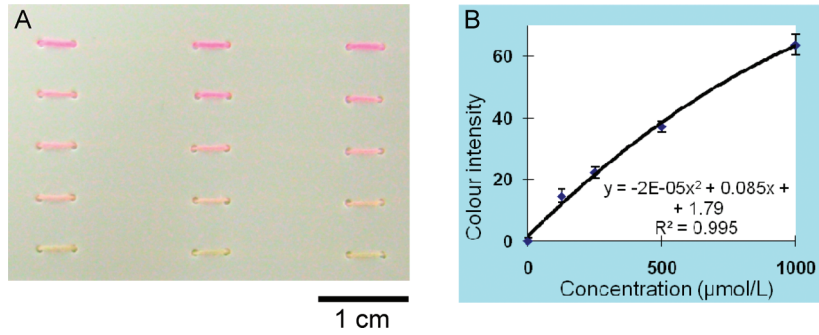

FIGURE 4. (A) Three parallel colorimetric measurements of serially diluted NO_2^- solution samples (0, 125, 250, 500, and 1000 μM) on the thread-based sensor. (B) NO_2^- concentration calibration curve established from thread stitches of six thread sensors using a desktop scanner and Adobe PhotoShop.

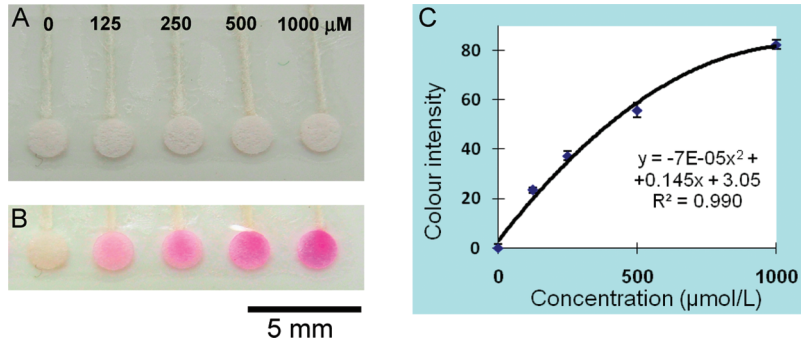

FIGURE 5. (A) Thread-paper microfluidic sensors using cotton thread as the liquid transport channel. (B) Colorimetric NO_2^- concentration series (0, 125, 250, 500, and 1000 μM) developed using a sensor array made of filter paper and cotton thread. (C) NO_2^- concentration calibration curve established from six thread-paper microfluidic sensors using a desktop scanner and Adobe PhotoShop.

Thread can also be used with other porous materials such as paper for semiquantitative colorimetric assay. Figure 5 shows a thread-paper microfluidic sensor array of a separate-sample-inlet design. Five NO_2^- indicator-treated paper discs were first laid onto a single-sided sticky tape in a line. Five hydrophilic cotton threads were then laid onto the sticky tape, each touching one of the five separate paper discs. A white opaque polymer film was finally pressed onto the sticky tape, forming the whole sensor. It is worth noting that using polymer film and sticky tape to form a sensor has an advantage of reducing sensor contamination and sample evaporation. NO_2^- solutions (0.8 μL) of a series of concentrations (0, 125, 250, 500, and 1000 μmol/L) were introduced in sequence using the micro pipet to the free end of each thread. The sample solutions rapidly penetrated along the threads and reached the paper discs in less than 2 s and triggered full color changes within 5 s. The fully developed colors were recorded by the digital camera for visual appraisal (Figure 5B) and by the desktop scanner for data analysis. The NO_2^- concentration calibration curve was established following the procedure mentioned earlier for thread-based sensors (Figure 5C). The circular area enclosing the entire paper disk was selected for color analysis, and six independent measurements were taken from the six thread-paper sensors to give the average values ± s.d.

Conclusions. Thread has been used to fabricate 3D and semiquantitative microfluidic analytical devices. An advantage of using thread as the liquid transporting channels is that it does not need patterned barriers. Another advantage of using thread or thread with other porous materials such as paper to fabricate microfluidic devices is that these devices can be fabricated with basic tools; the reliance on modern equipment is reduced. Certain simple devices may even be fabricated by a skilled work force within the textile industry in developing regions. It can be envisaged that thread, either alone or with other materials, can be used to fabricate a family of microfluidic diagnostic devices suitable for colorimetric, electrochemical, chemiluminescent, electrochemiluminesent assays and electrophoresis. The low-cost, flexible, and versatile nature of thread will allow this ancient material to have new applications in disposable microfluidic devices, advanced textile and personal care products, healthcare, and environmental sensors.

Acknowledgment. The research scholarships of Monash University and the Department of Chemical Engineering are gratefully acknowledged. The authors thank Dr. L. Wang of the School of Fashion and Textiles, RMIT University, for kindly providing us with the cotton thread sample, and Dr. T. Gengenbach of CSIRO Molecular and Health Technologies for taking XPS measurements of the thread samples. The authors specially thank Dr. E. Perkins of the Department of Chemical Engineering, Monash University, for proofreading the manuscript.

REFERENCES AND NOTES

(1) Weigl, B.; Domingo, G.; LaBarre, P.; Gerlach, J. *Lab Chip* **2008**, *8*, 1999–2014.
(2) Martinez, A. W.; Phillips, S. T.; Butte, M. J.; Whitesides, G. M. *Angew. Chem., Int. Ed.* **2007**, *46*, 1318–1320.
(3) Abe, K.; Suzuki, K.; Citterio, D. *Anal. Chem.* **2008**, *80*, 6928–6934.
(4) Li, X.; Tian, J.; Nguyen, T.; Shen, W. *Anal. Chem.* **2008**, *80*, 9131–9134.

(5) Fenton, E. M.; Mascarenas, M. R.; Lo'pez, G. P.; Sibbett, S. S. *ACS Appl. Mater. Interfaces* **2009**, *1*, 124–129.
(6) Carpi, F.; Rossi, D. D. *IEEE Trans. Inf. Technol. Biomed.* **2005**, *9*, 295–318.
(7) Paradiso, R.; Loriga, G.; Taccini, N. *IEEE Trans. Inf. Technol. Biomed.* **2005**, *9*, 337–344.
(8) Shim, B. S.; Chen, W.; Doty, C.; Xu, C.; Kotov, N. A. *Nano Lett.* **2008**, *8*, 4151–4157.
(9) Zhang, M.; Atkinson, K. R.; Baughman, R. H. *Science* **2004**, *306*, 1358–1361.
(10) Blicharz, T. M.; Rissin, D. M.; Bowden, M.; Hayman, R. B.; DiCesare, C.; Bhatia, J. S.; Grand-Pierre, N.; Siqueira, W. L.; Helmerhorst, E. J.; Loscalzo, J.; Oppenheim, F. G.; Walt, D. R. *Clin. Chem.* **2008**, *54*, 1473–1480.
(11) Nagler, R. M. *Clin. Chem.* **2008**, *54*, 1415–1417.
(12) Wink, D. A.; Kasprzak, K. S.; Maragos, C. M.; Elespuru, R. K.; Misara, M.; Dunams, T. M.; Cebula, T. A.; Koch, W. H.; Andrews, A. W.; Allen, J. S.; Keefer, L. K. *Science* **1991**, *254*, 1001–1003.
(13) Yager, P.; Domingo, G. J.; Gerdes, J. *Annu. Rev. Biomed. Eng.* **2008**, *10*, 107–144.
(14) Mabey, D.; Peeling, R. W.; Ustianowski, A.; Perkins, M. D. *Nat. Rev. Microbiol.* **2004**, *2*, 231–240.
(15) Hown-Grant, M. In *Encyclopedia of Chemical Technology*, 4th ed.; Wiley-Interscience: New York, 1993; Vol. 7, p 633.
(16) Vázquez, G.; Alvarez, E.; Navaza, J. M. *J. Chem. Eng. Data* **1995**, *40*, 611–614.
(17) Aspler, J. S.; Davis, S.; Lyne, M. B. *J. Pulp Paper Sci.* **1987**, *13*, 55–60.
(18) Nisbet, D. R.; Pattanawong, S.; Ritchie, N. E.; Shen, W.; Finkelstein, D. I.; Horne, M. K.; Forsythe, J. *J. Neural Eng.* **2007**, *4*, 1–7.
(19) Shaw, D. J. *Introduction to Colloid and Surface Chemistry*, 4th ed.; Butterworth: Oxford, U.K., 1992, p 71.
(20) Martinez, A. W.; Phillips, S. T.; Whitesides, G. M. *Proc. Natl. Acad. Sci. U.S.A.* **2008**, *105*, 19606–19611.

AM9006148